# Biosorption of Pb(II) from contaminated water onto *Moringa oleifera* biomass: kinetics and equilibrium studies

Muhammad Imran, Kamran Anwar, Muhammad Akram, Ghulam Mustafa Shah, Iftikhar Ahmad, Noor Samad Shah, Zia Ul Haq Khan, Muhammad Imtiaz Rashid, Muhammad Nadeem Akhtar, Sajjad Ahmad, Muhammad Nawaz & Ruud J. Schotting

Taylor & Francis
Taylor & Francis Group

Check for updates

# Biosorption of Pb(II) from contaminated water onto *Moringa oleifera* biomass: kinetics and equilibrium studies

Muhammad Imran[a,b], Kamran Anwar[a], Muhammad Akram[a], Ghulam Mustafa Shah[a], Iftikhar Ahmad[a], Noor Samad Shah[a], Zia Ul Haq Khan[a], Muhammad Imtiaz Rashid[c], Muhammad Nadeem Akhtar[d], Sajjad Ahmad[a], Muhammad Nawaz[e], and Ruud J. Schotting[f]

[a]Department of Environmental Sciences, COMSATS University Islamabad, Vehari, Pakistan; [b]MOE Key Laboratory of Pollution Process and Environmental Criteria, College of Environmental Science and Engineering, Nankai University, Tianjin, China; [c]Center of Excellence in Environmental Studies, King Abdulaziz University, Jeddah, Saudi Arabia; [d]Department of Chemistry, University of Agriculture, Faisalabad, Pakistan; [e]Center for Advanced Studies in Physics, GC University, Lahore, Pakistan; [f]Environmental Hydrogeology Research Group, Department of Earth Sciences, Utrecht University, Utrecht, Netherlands

## ABSTRACT

The present study aims at evaluating a batch scale biosorption potential of *Moringa oleifera* leaves (MOL) for the removal of Pb(II) from aqueous solutions. The MOL biomass was characterized by FTIR, SEM, EDX, and BET. The impact of initial concentrations of Pb (II), adsorbent dosage, pH, contact time, coexisting inorganic ions ($Ca^{2+}$, $Na^+$, $K^+$, $Mg^{2+}$, $CO_3^{2-}$, $HCO_3^-$, $Cl^-$), electrical conductivity (EC) and total dissolved salts (TDS) in water was investigated. The results revealed that maximum biosorption (45.83 mg/g) was achieved with adsorbent dosage 0.15 g/100 mL while highest removal (98.6%) was obtained at adsorbent biomass 1.0 g/100 mL and pH 6. The presence of coexisting inorganic ions in water showed a decline in Pb(II) removal (8.5% and 5%) depending on the concentrations of ions. The removal of Pb(II) by MOL decreased from 97% to 89% after five biosorption/desorption cycles with 0.3 M HCl solution. Freundlich model yielded a better fit for equilibrium data and the pseudo-second-order well described the kinetics of Pb(II) biosorption. FTIR spectra showed that –OH, C–H, –C–O, –C=O, and –O–C functional groups were involved in the biosorption of Pb(II). The change in Gibbs free energy ($\Delta G = -28.10$ kJ/mol) revealed that the biosorption process was favorable and thermodynamically driven. The results suggest MOL as a low cost, environment-friendly alternative biosorbent for the remediation of Pb(II) contaminated water.

## KEYWORDS

Biosorption; characterization; equilibrium; kinetics; *Moringa oleifera*; reusability

## Introduction

Heavy metals (HMs) are natural constituents of the Earth's crust and differ in their solubility, mobility, bioavailability, and toxicity (Shahid *et al.* 2018). Consumption of HMs contaminated food is the major pathway for human exposure (Xiong *et al.* 2016). The HMs have become a serious global issue and their concentration in wastewater and drinking water exceeds the permissible limits (Ahmed and Mustafa 2008; Shahid *et al.* 2018). These hazardous chemicals can enter the human body through food (65%), water (20%), and air (15%) (Adeogun *et al.* 2010). Long-term exposure to heavy metals results in death due to their noxious nature (Sulaymon *et al.* 2013; Gao *et al.* 2017). Lead is one of the toxic heavy metals that readily gets collected in the human body (Carolin *et al.* 2017) and is recognized as the 36th most abundant component of the Earth's crust (John 2011).

Lead exists naturally in the form of cerussite, sulfide, and galena (Acharya *et al.* 2009; Carolin *et al.* 2017). The anthropogenic sources contributing to lead accumulation in the environment include electrical industries, lead-acid battery, electroplating, painting, explosive manufacturers, photographic materials, aeronautical, and steel ventures (Igbal and Edyvean 2004; Carolin *et al.* 2017). The threshold level for Pb(II) in wastewater set by the Environmental Protection Agency (EPA-USA) is 0.05 mg/L and in drinking water set by the EU and WHO are 0.01 and 0.015 mg/L, respectively (Balaria *et al.* 2008). Consequently, it is imperative to remove Pb(II) from wastewater before its consumption.

There are various strategies to remove Pb(II) from wastewater and modern effluents including osmosis, electrodialysis, extraction, film filtration, precipitation, carbon adsorption, and ion exchange electrolysis (Pappalardo *et al.* 2010; Anastopoulos *et al.* 2013; Bilal *et al.* 2013; Suganya and Kumar 2018a). All these traditional remediation strategies are effective but not accepted in the society either due to high cost or sludge production. Industrial byproducts are

used as low-cost adsorbents including pulp, paper, sugarcane bagasse, steelmaking slag, fly ash bagasse, seeds and leaves of trees, etc. (Soliman et al. 2011; Tofan et al. 2011; Yao et al. 2012; Shakoor et al. 2015; Abid et al. 2016; Ahmad et al. 2017). Low-cost nonagricultural adsorbents such as peat, clay, natural zeolites, aragonite shells and lignin are also used for water treatment (Liu et al. 2008). However, the removal of Pb(II) from aqueous systems by adsorption using biomass has proved to be very effective in terms of metal removal and cost efficiency. Biosorption has received significant attention because of its minimal effort and environment-friendly nature (Chandrasekhar et al. 2001). Selection of the most suitable adsorbent material depends on its technical applicability and cost-effectiveness. The plant biomass like leaves, flowers, bark, and pods contains a large amount of lignin, cellulose, and hemi-cellulose, which are composed of C, H, and N contents. These materials have a great tendency to adsorb positively charged heavy metals like Pb(II) (Tarley and Arruda 2004). Most of the biomasses like compost, biochar, rice husks, wheat straw, tea leaves, peanut skins, pines bark and coconut husk are composed of cellulose, hemicelluloses, pectin, and lignin with a small amount of protein (Demirbas 2008; Wang and Chen 2009; Shakoor et al. 2015; Abid et al. 2016; Ahmad et al. 2017; Niazi et al. 2018). The biomasses of Asplenium nidus (Dissanayake et al. 2016), lemongrass (Babarinde et al. 2016), apple juice and tomato waste (Heraldy et al. 2018), Solanum melongena leaf (Yuvaraja et al. 2014), and Moringa oleifera seed powder (Adhiambo et al. 2015; Aziz et al. 2016) were used for the removal of Pb(II) from contaminated water.

Moringa (Moringa oleifera L.) also known as the miraculous tree (evergreen) is widely distributed in tropical areas having enough tolerance to drought and is easily available in Pakistan. It has a number of applications in the medical field, for example, anti-inflammatory, antihypertensive activity and analgesic, weight losses, etc. Moringa oleifera leaves (MOL) are rich in protein, vitamin C, potassium, and calcium (Anwar et al. 2007). Moringa seeds were used by Ravikumar and Sheeja (2013) for the removal of cadmium, copper, chromium, and lead from drinking water and its seed ash was effectively used by Dobaradaran et al. (2015) for the removal of fluoride from aqueous solutions. Moringa seeds proved as a very effective biosorbent for the remediation of heavy metals (Araújo et al. 2010, 2013). Tavares et al. (2017) used husks, pods, and seeds of Moringa oleifera for the removal of Pb(II) from contaminated water. The bark of Moringa oleifera was used by Reddy et al. (2011) for the removal of Ni from aqueous solutions as a low-cost biosorbent and was proved to be very effective. Matouq et al. (2015) used Moringa aptera Gaertn (MAG) to evaluate its effectiveness for the removal of copper, nickel, chromium, and zinc ions from synthetic wastewater.

To the best of our knowledge, Moringa oleifera leaves (MOL) have not been used for remediation of Pb(II) from contaminated water so far. So, the present study is aimed at using MOL as a natural biosorbent for the removal of Pb(II) from contaminated water at batch scale and get it characterized. The reusability and efficiency of MOL have also been investigated. The effect of process parameters: pH, the initial concentration of Pb (II), the dosage of MOL, contact time, and presence of competing ions on the removal of Pb(II) from contaminated water has been evaluated. In the end, experimental results were validated with equilibrium isotherms (Langmuir, Freundlich, Temkin, and Dubinin-Radushkevich) and kinetic models (pseudo first order, pseudo second order, Elovich, and Intra-particle diffusion). The biosorption potential of MOL was compared with other parts of Moringa oleifera and other biosorbents previously used for Pb(II) removal.

## Materials and methods

### Preparation and processing of Moringa oleifera biomass

Moringa oleifera leaves (MOL) were collected from COMSATS University Islamabad, Vehari Campus and were washed thoroughly with distilled water to remove the adhering dirt and particulate material. The washed leaves were air-dried and then oven dried at 70 °C for 20 h. The dried biomass was ground to a fine powder using a blender. The powder was also washed repeatedly with distilled water until the water became clear. The powder was oven dried at 65 °C for 24 h and stored in a plastic container for further application. No other chemical or physical treatment was applied prior to the adsorption experiments.

### Characterization of MOL adsorbent

The characterization of the biosorbent is very important for understanding the biosorbent-metal interaction and biosorption mechanism. The surface area, pore size distribution, and pore volume were measured using Brunauer–Emmett–Teller (BET, Tristar II 3020, Micromeritics, Houston, Texas). The sample was degassed followed by the adsorption–desorption processes using nitrogen. The distribution of the main active functional groups possibly involved in the removal of Pb(II) was determined with Fourier Transform Infrared Spectroscopy (FTIR, Thermo Scientific Nicolet 6700, Madison, WI) in the range of wavenumber 500–4000 cm$^{-1}$. The micrographs for the morphology of the particles surface were obtained with Scanning Electron Microscopy (SEM) using a JEOL JSM-6480 (JEOL, Tokyo, Japan) scanning electron microscope equipped with an energy dispersive X-ray spectrometer (EDX). The morphological studies and elemental composition were performed at 20 kV. Energy dispersive X-ray spectroscopy (EDX) is an analytical technique employed to evaluate the elemental composition of a sample (Kaveeshwar et al. 2018). EDX was carried out for both samples of MOL to evaluate the involvement of MOL in Pb(II) biosorption thereby measuring the elemental composition of the material.

### Reagents and preparation of the synthetic solution

The chemicals used in the experiment were of analytical grade. A standard solution of Pb(II) with a concentration of 1000 mg/L was prepared by dissolving 1.6 g of lead nitrate

(Pb (NO$_3$)$_2$) in 1 L distilled water. The various concentrations of Pb(II) (5, 10, 20, 40, 80, and 160 mg/L) were prepared through dilution of the standard solution and were used in the batch study. The pH of the solution was adjusted with 1 M NaOH or HCl solutions using a pH meter (Milwaukee pH55, Milwaukee, Thailand).

## Measurement of the point of zero charge of MOL

The point of zero charge (PZC) of MOL was measured by using an electrolyte solution (Aliabadi et al. 2018). About 0.1 M NaCl solution was prepared in distilled water and separated in different conical flasks. The pH of NaCl solution in flasks was adjusted to 4, 6, 8, 10, and 12 using 0.1 M NaOH and HCl. A dosage of 0.1 g of MOL was added in each flask. For control, five flasks of pH 4, 6, 8, 10, and 12 were used without MOL. All these flasks were kept on a mechanical shaker at 150 rpm for 24 h. Next day, the samples were filtered and their pH was measured. A graph was plotted between initial pH (4, 6, 8, 10, and 12) and final pH after interaction of the material with an electrolyte solution. The point of intersection of the curve of the control and curve with MOL pH gave PZC.

## Biosorption experiments

A series of biosorption experiments for evaluating the affinity of adsorbent (MOL) for Pb(II) sorption was performed in duplicate sets in 250 mL flasks containing 100 mL of Pb(II) solution. The biosorption capacity of MOL was determined at various initial concentrations of Pb(II) ranging from 5 to 160 mg/L. The samples were taken after 15, 30, 60, 120, and 180 min until equilibrium was reached to measure the concentration of Pb(II) in the solution. The water samples were agitated at 200 rpm with a rotary shaker and centrifuged at 3000 rpm for 10 min at room temperature. The samples were filtered and residual concentration of Pb(II) was measured with Atomic Absorption Spectrophotometer (AAS, Agilent AA240, Agilent, CA, USA).

## Effect of adsorbent dosage

It is important to optimize the amount of the adsorbent material for the removal of metal ions as it plays a direct role in the overall cost of the adsorption system (Nithya et al.

2018). The effective dosage of the biosorbent for the removal of Pb(II) was determined by varying the amount of MOL from 0.15–1.0 g/100 mL keeping other parameters constant. A measured quantity of MOL was taken in 100 mL Pb(II) solution at constant pH 6 (optimum) and initial concentration of Pb (5–160 mg/L). The effective dosage was chosen on the basis of Pb(II) removal (%) at different dosage of MOL.

## Effect of time and pH

The effect of time on Pb(II) removal was evaluated at fixed pH (6) and an MOL dosage of 0.7 g/100 mL (optimum dosage) varying Pb concentration from 5–160 mg/L. The samples were agitated on a rotary shaker and collected after 15, 30, 60, 120, and 180 min. While to determine pH effect, pH was varied from 2–10 and other factors: initial concentration of 40 mg/L, dosage of 0.7 g/100 mL, and room temperature were kept constant based on the preliminary studies.

## Impact of inorganic ions on Pb(II) sorption

In order to investigate the interference resulting from the presence of inorganic ions in solution on the removal of Pb(II) from contaminated water, two groundwater samples were taken from two different places of District Vehari; one from Burewala and other from Vehari city were used. Groundwater samples were analyzed for inorganic ions (Na$^+$, Ca$^{2+}$, Mg$^{2+}$ and K$^+$, CO$_3$$^{2-}$, HCO$_3$$^-$), EC using EC meter (Lovibond SensoDirect 150, Lovibond, Berlin, Germany), TDS using TDS meter (HI98301 DiST 1), Cd and As to evaluate their impact on the removal of Pb(II) from aqueous systems. Solutions of four different initial concentrations of Pb(II) (10, 20, 40, and 80 mg/L) in groundwater samples were prepared through dilution of the standard solution keeping in view the initial concentration of Pb(II) in groundwater (Table 1). This set of experiments was carried out at MOL dosages of 0.15 and 0.7 g/100 mL in each groundwater sample.

## Data analysis

The data used in the analysis are means of duplicate sets of experiments. The amount of adsorbed Pb(II) per unit mass of the *Moringa oleifera* leaves q (mg/g) was determined by measuring the final concentration of the Pb(II) (mg/L) in

**Table 1.** Isotherm and kinetic models constants for the adsorption of Pb(II) by MOL at adsorbent dosage 0.7 g/100 mL, room temperature, initial Pb(II) concentration 80 mg/L and pH 6.at adsorbent dosage 0.7 g/100 mL, room temperature, pH 6.

**Equilibrium models parameters**

| Langmuir | | | Freundlich | | | Temkin | | | Dubinin-Radushkevich | | | |
|---|---|---|---|---|---|---|---|---|---|---|---|---|
| $K_L$ | $q_{max}$ | $R^2$ | $K_F$ | $n$ | $R^2$ | $K_T$ | $b$ | $R^2$ | $q_m$ | $B$ | $E$ | $R^2$ |
| 0.078 | 14.124 | 0.94 | 1.558 | 2.1 | **0.995** | 1.636 | 5496 | 0.831 | 4.54 | 6.86E-02 | 2.7 | 0.55 |

**Kinetic models parameters**

| Pseudo first order | | | Pseudo-second order | | | Elovich | | | Intra-particle diffusion | | |
|---|---|---|---|---|---|---|---|---|---|---|---|
| $q_e$ | $k_1$ | $R^2$ | $q_e$ | $k_2$ | $R^2$ | $\alpha$ | $\beta$ | $R^2$ | $k_{id}$ | $a$ | $R^2$ |
| 7.31 | 0.121 | 0.975 | 9.1 | 0.005 | **0.996** | 4.585 | 0.485 | 0.94 | 0.573 | 2.064 | 0.86 |

The bold numbers indicate the R2 value of the model which is more suitable in kinetic and equilibrium adsorption.

the solution $C_f$, volume (L) of the solution $V_w$, initial concentration of Pb(II) ($C_0$) in the solution (mg/L) and mass of the biosorbent material $M_b$ (g) following Eq. (1) (Kołodyńska et al. 2017).

$$q = \frac{(C_0 - C_f)}{M_b} \times V_w \qquad (1)$$

The metal removal efficiency (R%) by the biosorbent from solution was calculated by Eq. (2) (Ahmad et al. 2017)

$$R\ (\%) = \left(\frac{C_0 - C_f}{C_0}\right) \times 100 \qquad (2)$$

## Adsorption kinetics and isothermal study

The isothermal experimental data were analyzed and validated with Langmuir, Freundlich, Temkin, and Dubinin–Radushkevich isotherm models. Suitability of adsorption isotherm models was evaluated on the basis of coefficient of determination ($R^2$) and Chi-squared test using Eq. (3) (Niazi et al. 2018).

$$\chi = \sum \left[\frac{(q_e - q_{cal})^2}{q_{cal}}\right] \qquad (3)$$

Where $q_{cal}$ is the adsorption capacity (mg/g) calculated from the models and $q_e$ is the experimental adsorption capacity.

To evaluate kinetics: pseudo-first order, pseudo-second order, Elovich, and intra-particle diffusion models were employed for biosorption experiments. Gibbs free energy for the biosorption process was calculated following Saha et al. (2017). Moreover, the sorption potential of Pb(II) by MOL was compared with the potential of other biosorbents and other parts of *Moringa oleifera* used in the literature.

## Desorption process and reusability of the biosorbent

Experiments were conducted for the desorption of Pb(II) from air dried Pb(II) loaded MOL (0.15 g/50 mL) to the solution using 0.1, 0.2 and 0.3 M HCl. The adsorption–desorption experiments were repeated in five cycles.

The metal desorption (recovery %) from biosorbent surface to the solution was calculated with Eq. (4) (Kołodyńska et al. 2017).

$$Recovery\ (\%) = \frac{C_{des}}{C_{ads}} \times 100 \qquad (4)$$

Where $C_{des}$ is the desorbed concentration and $C_{ads}$ is the adsorbed concentration of the metal ions.

## Results and discussion

### Characterization of the particles derived from Moringa oleifera leaves

The surface characterization of the biosorbent is very important for understanding the biosorbent-metal interaction and biosorption mechanism. FTIR spectroscopy was used to identify the functional groups on MOL surface and interaction of the biosorbent with Pb (II). The data obtained from FTIR spectrum of MOL before and after Pb(II) adsorption showed the differences in the absorbance peaks of different functional groups (Figure 1(a)). Tarley and Arruda (2004) found that plant biomass like leaves, flowers, bark, and pods contain a large amount of lignin, cellulose, and hemicellulose giving various functional groups. These materials have a great tendency to adsorb positively charged heavy metals (Ali et al. 2016). The variation in peak values of absorbance is due to the interaction between functional groups present on MOL and the target contaminant (Al-Ghouti et al. 2003). The shifts in the spectra showed that MOL is a useful biosorbent in the removal of heavy metal ions. It was also observed that absorbance peaks at 1010, 1020, 1220 cm$^{-1}$, and 1230 cm$^{-1}$ show the presence of –C–O functional groups. The absorbance of MOL at 1620–1630 cm$^{-1}$ represents –C=O groups while absorbance peaks at wavenumber 2330–2360 cm$^{-1}$ indicate symmetry of –C≡C– (Bueno et al. 2008). Similarly, the absorbance peaks at 2900–2910 cm$^{-1}$ indicate C–H bonds of methyl, methylene, and methane. In Figure 1(a), O–H stretching is observed at 3290 cm$^{-1}$ and 3310 cm$^{-1}$ on the surface of MOL. Moreover, *cis*=C–H out-of-plane bending is observed at wavenumber 651–661 cm$^{-1}$. The presence of such functional groups can also be justified from the studies conducted by Iqbal and Bhanger (2006) and Sreelatha and Padma (2009). A higher variation in the spectra before and after Pb(II) attachment shows more interaction between the adsorbent surface and metal ion. The main groups contributing to Pb(II) sorption through MOL are –OH, C–H, –C–O, –C=O, and –O–C. The adsorption mechanism involved in the Pb removal with MOL having the aforementioned functional groups has been presented in Supplementary Figure 1.

The SEM images show the surface morphology of MOL before and after adsorption (Figure 1(b) and (c)). Some deformations on the surface of the leaf tissue can be observed, containing available sites and grooves to provide favorable conditions for the adsorption of metal species in the interstices (Reddy et al. 2011). The surface was rough and uneven before adsorption and became less heterogeneous with the attachment of Pb (II). These results are closely related with Al-Ghouti et al. (2003) who found that the pores on the surface were irregular and have great porosity for adsorption. Similar observations were also made by Hameed et al. (2007) who found that these pores provided a good surface for dyes and heavy metals adsorption (Bello and Ahmad 2011). These characteristics of the biosorbent have favored heavy metal adsorption (Araújo et al. 2010; Guiza 2017; Tavares et al. 2017). The average particle size measured with SEM was 50.7 μm

EDX results supported Pb(II) sorption onto MOL biosorbent. In Figure 2(a), Pb(II) was absent in pristine MOL whereas Pb(II) was present in loaded MOL (Figure 2(b)). It is observed that in pristine MOL, main elements were C and O and minor elements were Mg, S, K, Ca. But in Pb(II) loaded scenario, minor elements, completely, and some percentage of major elements were replaced with Pb (II).

**Figure 1.** FTIR spectra of *Moringa oleifera* leaves before (pristine) and after Pb(II) biosorption (a), SEM images of *Moringa oleifera* leaves at 10 μm resolution, pristine *Moringa oleifera* leaves (b), Pb(II) loaded *Moringa oleifera* (c).



**Figure 2.** EDX elemental composition of *Moringa oleifera* leaves, pristine *Moringa oleifera* leaves (a), Pb(II) loaded *Moringa oleifera* leaves (b), distribution of pore volume of MOL (c), isothermal linear plot of the Nitrogen adsorbed and desorbed as a function of relative pressure during BET analysis (d).

Brunauer-Emmett-Teller (BET) method was used to determine BET surface area and pore size distribution. $N_2$ gas was used in this method for circulation. The specific surface area of the MOL was 35.21 m$^2$ g$^{-1}$. Figure 2(c) gives pore size distribution in MOL biomass and Figure 2(d) presents pore volume (cm$^3$/g) as a function of relative pressure during BET analysis. It is observed that there is a steep increase is $N_2$ adsorption–desorption in the beginning and at the end as a function of relative pressure. Furthermore, there is variation in adsorption and desorption curves.
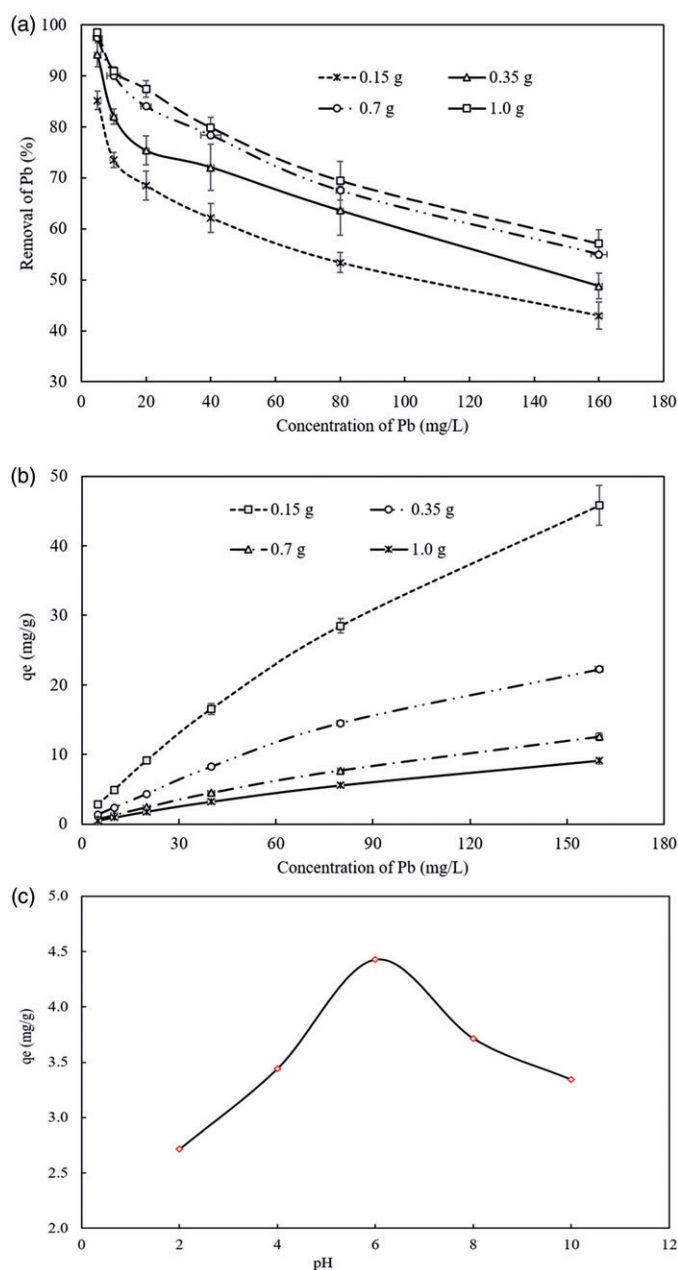
## Effect of initial concentration of Pb(II) and dosage of MOL

The lead contamination of water is one of the most important threats to water resources as well as to human health. Several biomasses have been evaluated as metal adsorbent material (Wang and Chen 2009) but the present study has been designed to evaluate the potential of MOL for the removal of Pb(II) from contaminated water. Figure 3(a) reveals that removal (%) of Pb(II) is decreased with increase in Pb(II) concentration which is attributed to the higher number of metals ions at a higher concentration than the active sites at a given dosage. These results are in close agreement with the findings of Ahalya et al. (2005). It is reported that the saturation of the biosorbent surface depends on the initial concentration of metal (Babarinde et al. 2016; Nadeem et al. 2016). Moreover, Figure 3(b) shows that the amount of Pb(II) ions adsorbed per unit mass of the adsorbent (MOL) increases as Pb(II) concentration is increased from 5–160 mg/L at a fixed dosage of the adsorbent

For a given solution, the adsorption process is affected by the dosage of adsorbent in aqueous solution at fixed initial concentration and time. The dosage of the material must be optimized for maximum removal of the contaminant. In the present study, biosorption and removal of Pb(II) onto MOL were studied by changing its dosage from 0.15 to 1.0 g/100 mL at all initial concentrations (5–160 mg/L), pH 6 and room temperature. It was observed that with an increase in mass of MOL, removal of Pb(II) from aqueous solution is also increased (Figure 3(b)) beyond which there is a minimum change in adsorption and removal of Pb (II). The increase in Pb(II) removal efficiency with increasing adsorbent dosage may occur due to more number of active sites and higher surface area of the biosorbent at an increased dosage. The maximum removal (98.6%) occurred at 1.0 g/100 mL aqueous solution, whereas minimum at 0.15 g/100 mL. There was more difference in Pb(II) removal and biosorption when dosage changed from 0.15–0.7 g, further increase in biosorbent dosage did not bring any further improvement in Pb(II) removal by MOL (Figure 3(b)) due to aggregation of the particles (Ahmad et al. 2017). So, the optimum dosage for Pb(II) removal with MOL was 0.7 g/100 mL.

## Effect of pH

The pH of the water, the particle size of biosorbent, temperature, ionic strength, presence of competitive inorganic ions, stirring time, and dosage of the adsorbent are the



Figure 3. Effect of initial concentration of Pb(II) and dosage of MOL on the removal (a) and biosorption of Pb(II) from aqueous systems (b), effect of pH on Pb (II biosorption when initial concentration of the Pb(II) is 40 mg/L and dosage of MOL is 0.7 g/100 mL at room temperature (c).

factors controlling the removal of the target contaminants (Araújo et al. 2013; Nadeem et al. 2016).

The solution pH is a critical variable controlling the biosorption process for the removal of contaminants from aqueous solution (Reddy et al. 2012). The impact of solution pH on Pb(II) removal was determined at Pb(II) concentration, 40 mg/L, 0.7 g MOL/100 mL and the selected pH values were: 2, 4, 6, 8, and 10. The maximum Pb(II) biosorption was observed in the range of 4–6 pH (Figure 3(c)). A similar trend of Cd, Cu, and Ni biosorption as a function of solution pH was observed by Reddy et al. (2012) in which they used chemically modified MOL for the removal of Ni from aqueous solution. Further increase in pH decreases metal ion removal from the solution. This change in Pb(II)
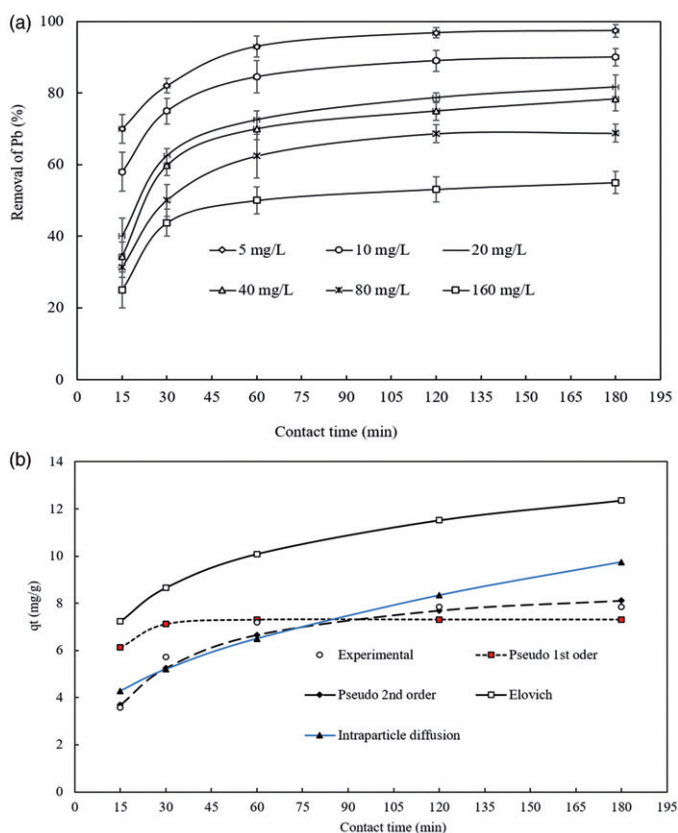
**Figure 4.** Evolution of equilibrium at different initial concentrations of Pb(II) in the solution at adsorbent dosage 0.7 g/100 mL, pH 6 and room temperature (a), comparison of experimental kinetic adsorption with calculated kinetic adsorption from four different kinetic models (b).

removal due to pH variation can be attributed to different functional groups present on the biosorbent surface involved in the removal process. The pH effect at lower and higher pH values can be explained with the competition between $H_3O^+$ and metal ions in the solution. There is a decline in $H_3O^+$ at higher pH which favors occupation of sorption sites by metal Pb (II). While at low pH, $H_3O^+$ increases and has a negative effect on the removal of other positively charged ions by the biosorbent surface. Reddy et al. (2012) found a point of zero charge (PZC), which was a pH of $3.72 \pm 0.21$ in case of modified MOL for the removal of Cd, Ni, and Cu. In our case, the PZC of MOL is 5.5±.0.24, which can be used to explain the impact of pH. The removal of metals by biosorbent is favored when pH > PZC, thereby increasing negatively charged sites and is deceased when pH < PZC due to the presence of more positively charged ions in solution at low pH discouraging metals removal. Maximum removal of Pb(II) was attained at pH 6 (Figure 3(c)). Similarly, maximum Pb(II) removal was obtained at pH 6 by Tavares et al. (2017) using husks, pods, and seeds of *Moringa oleifera*.

### Effect of contact time

Contact time is one of the major factors controlling biosorption and removal of metal ions. Figure 4(a) shows the effect of contact time (15, 30, 60, 120, and 180 min) on Pb(II)

removal at initial concentrations 5–160 mg/L, fixed dosage 0.7 g/100 mL and pH 6. It is observed that Pb(II) removal percentage increases sharply with contact time (0–15 min) due to a large number of vacant active adsorption sites available in the beginning. Sharpness in the removal of Pb(II) is decreased with time (15–60 min). After 60 min, the Pb(II) removal curves becomes almost constant, which shows that the point of equilibrium is reached. This occupation of available sites causes no more change in removal efficiency with increase in time due to saturation of adsorption sites. The results revealed that maximum Pb(II) was removed in first 60 min (Figure 4(a)). Sheng et al. (2005) also observed that adsorption of lead, copper, cadmium, zinc, and nickel occurred within 60 min. According to Sarada et al. (2014), contact time of 1 h is optimum for the biosorption of Pb(II) ions from industrial wastewater using different biomasses.

### Impact of the inorganic ions

The presence of coexisting ions in the aqueous system may interfere in metal removal by biosorbents (Reddy et al. 2011; Vilvanathan and Shanthakumar 2015). Therefore, it is important to investigate the influence of inorganic ions (e.g. sodium, potassium, calcium, magnesium), EC and TDS on the removal of Pb(II) from the solution by the biosorbent. The cations are the major constituents generally encountered in the remediation of metals from contaminated water. Two groundwater samples (GW1 and GW2) with characteristics given in Supplementary Table 1 were used to analyze the impact of cations ($Ca^{2+}$, $Na^+$, $K^+$, $Mg^{2+}$), anions ($CO_3^{2-}$, $HCO_3^-$, $Cl^-$), EC and TDS on the biosorption and removal of Pb(II) from the solution. Figure 5(a) shows the removal of Pb(II) by the biosorbent in the presence of ions given in Supplementary Table 1 at equilibrium. Electrical conductivity gives information on the presence of different salts in water. Therefore, two different groundwater samples with different characteristics were used to investigate the removal of Pb(II) in the presence of different ions. The results reveal that increasing the concentration of cations, EC and TDS in the groundwater samples decrease biosorption potential of the material and removal of Pb (II). The biosorbent dosage 0.15 g showed more decline in biosorption and removal (8.5% and 5% with GW1, GW2, respectively) as compared with dosage 0.7 g (6% and 4% with GW1, GW2, respectively). This may occur due to the poor affinity of $Na^+$ and $K^+$ ions with Pb(II) as compared with an affinity of $Ca^{2+}$, $Mg^{2+}$ ions (Meseguer et al. 2016). The values of the parameters were relatively greater for GW1 than GW2. This finding agrees with Meseguer et al. (2016) who also reported similar results in synthetic contaminated water. But, in our case, all the cations and anions given in Supplementary Table 1 were present at the same time in water samples. Nevertheless, Reddy et al. (2012) reported non-significant effects of cations on the biosorption potential of modified MOL for Cd, Ni, and Cu using salts of the respective cations individually in each metal solution. In another study by Reddy et al. 2011, the impact of $Ca^{2+}$ and $Mg^{2+}$ on the Ni ions removal
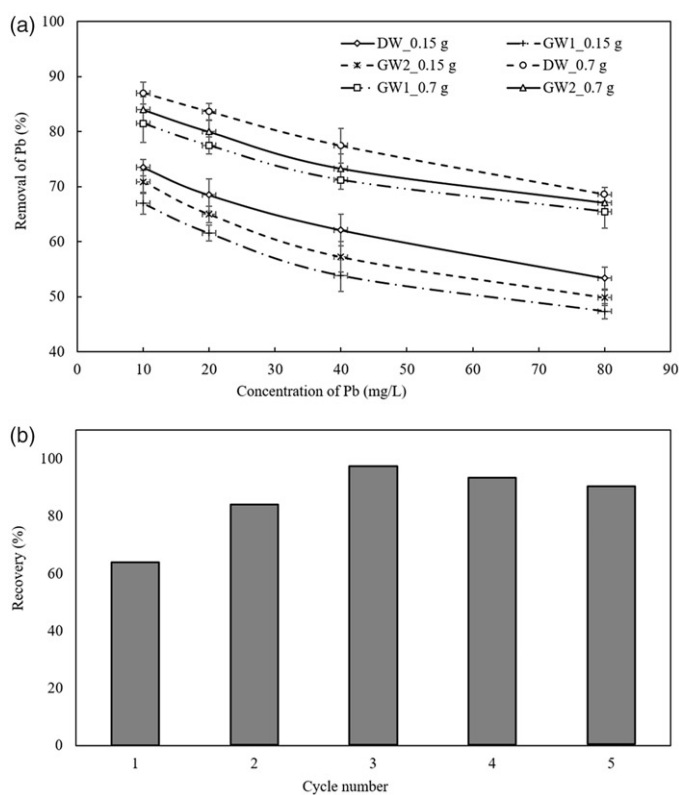
**Figure 5.** Effect of inorganic ions, EC and TDS on the removal of Pb(II) from the contaminated water at room temperature, two different dosages of the biosorbent (0.15 and 0.7 g/100 mL). DW represents distilled water and GW indicates groundwater sample (a), recovery of the metal ions for reusability of MOL using HCl (0.1–0.3 M) with 5 cycles (b).

was marginal but higher than monovalent cations (Na$^+$, K$^+$). Our results suggest that MOL performs better in the removal of Pb(II) from aqueous systems where less concentration of Ca$^{2+}$ and Mg$^{2+}$ is present than their elevated levels in water. Moreover, in future, the efficiency of MOL biomass can be improved with physical and chemical treatments and composites of MOL biomass with nanoparticles.

## Desorption study for reusability of the MOL

In biosorption study, it is important to keep processing cost low thereby improving the recovery of the biosorbent material for its reuse. To evaluate the feasibility of MOL biosorbent for its reuse efficiency, experiments for the desorption of Pb(II) from Pb(II) loaded MOL (54.87 mg/L adsorbed per 0.7 g) to the solution were conducted using 0.1, 0.2, 0.3, 0.35, and 0.4 M HCl (Figure 5(b)). Treatment of metal loaded biosorbent with HCl is efficient for desorption of metals for reusability of the biosorbent (Saeed and Iqbal 2003; Reddy et al. 2011). The maximum recovery of the biosorbent was 97.1% with 0.3 M HCl. The results showed that there was an increase in the recovery (%) with an increase in the concentration of HCl solution (0.1–0.3 M). Further increase (0.35, 0.4 M) in HCl concentration did not change recovery due to the stable behavior of the biosorbent. Reddy et al. (2011) used the bark of *Moringa oleifera* for the biosorption of Ni from the aqueous systems and

obtained 98.20% recovery of the material with 0.2 M HCl. The regenerated MOL material was reused for biosorption of Pb(II) from the solution. There was a gradual decline in the biosorption capacity of MOL with an increase in the number of cycles. In the present study, the removal of Pb(II) from solution to the MOL surface decreased from 97% to 89% after five biosorption/desorption cycles. There was an 8% decline in the Pb(II) removal by MOL from an aqueous solution which might be attributed to the removal of MOL biomass with 0.3 M HCl solution used for desorption study.

## Study of equilibrium models for biosorption

Testing of solid–liquid adsorption system is preliminary based on two types of studies: (a) Equilibrium batch sorption studies (b) Dynamic continuous flow sorption studies. Modeling of equilibrium data plays a very important part in the biosorption process as it gives information for comparison of different biomaterials under different conditions and operational procedures (Benguella and Benaissa 2002). The equilibrium biosorption data were validated with Langmuir (Eq. 5), Freundlich (Eq.7), Temkin (Eq.8) and Dubinin-Radushkevish (Eq. 9) isotherm models. The values of the parameters of all these models are given in Table 1.

The Langmuir model is valid for monolayer adsorption with a limited number of identical sorption sites on the surface of the biosorbent, which depends on the active sites with uniform energy for adsorption. In the Langmuir model, all adsorption sites are equally capable of holding the metal (Pb (II)). In Eq. (5), the two parameters $Q_{max}$ and $q_e$ are unknown and their values were calculated from the linearized form of Eq. 5 (Subramani and Thinakaran 2017).

In the case of Langmuir biosorption isotherm, the favorability of the biomass for adsorption can be expressed in terms of a dimensionless constant separation factor $R_L$, which is defined in Eq. (6). In the Supplementary Figure 2, $R_L < 1$ indicates strongly favorable biosorption of Pb(II) on MOL (Mirghaffari et al. 2015). The values of $Q_{max}$ (14.12 mg/g) and $K_L$ (Table 1) were measured from the slope and intercept of the curve $C_e/q_e$ vs $C_e$ (Subramani and Thinakaran 2017).

$$\frac{C_e}{q_e} = \frac{1}{Q_{max}K_L} + \frac{1}{Q_{max}}C_e \qquad (5)$$

$$R_L = \frac{1}{1 + K_L C_0} \qquad (6)$$

Where $q_e$ is the metal adsorbed at equilibrium per unit mass of the biosorbent (mg/g), $K_L$ (L mg$^{-1}$) is a Langmuir sorption equilibrium constant related to affinity of the binding sites, $Q_{max}$ (mg g$^{-1}$) is the maximum amount of the Pb(II) adsorbed on *MOL* biomass and $C_{eq}$ is metal concentration in the solution (mg/L) at equilibrium, $C_0$ is the initial concentration of the metal in the solution (mg/L).

Gibbs free energy for biosorption was calculated using Langmuir constant ($K_L$) (Saha et al. 2017). The change in Gibbs free energy for biosorption process, *i.e.*

$\Delta G = -28.10$ kJ/mol which suggests that the biosorption process was favorable and was thermodynamically driven.

Freundlich isotherm model is another generally employed model for equilibrium adsorption isotherm assuming heterogeneous sorption surface (Eq. 7) (Shim et al. 2015; Imran et al. 2018).

$$\log q_e = \log K_F + \frac{1}{n} \log C_e \qquad (7)$$

Where $K_F$ is the Freundlich distribution coefficient or adsorption capacity and $1/n$ is an empirical parameter called Freundlich constant representing the medium heterogeneity and adsorption intensity (Kamal et al. 2010). The value of $n$ is usually larger than unity. More the value of $n$ is in the Freundlich model, more favorable is the adsorption and more will be the heterogeneous surface of the particles. The Freundlich parameters $K_F$ and $n$ are determined from the slope and intercept of the plot of $\log q_e$ vs $\log C_e$ (Shim et al. 2015). The Freundlich model is widely used in water/wastewater treatment but provides no information about the monolayer adsorption capacity (Raoof et al. 2010). It considers that the stronger adsorption sites are filled first and there is a decline in the binding energy of the adsorption sites with the degree of site occupation. High values of correlation coefficient ($R^2 = 0.995$) in Table 1 showed that Freundlich model better represented the biosorption of Pb(II) by MOL while Langmuir model ($R^2 = 0.94$) adequately fitted with the experimental equilibrium data. The MOL biomass has a rough and heterogeneous surface as observed during SEM analysis, which also favors the Freundlich model. The value of $n$ in Freundlich model is more than 2 which shows MOL as a good adsorbent (Nithya et al. 2018; Suganya and Kumar 2018a)

The Temkin isotherm model (Eq. 6) assumes that adsorption energy of all the molecules in a layer is reduced linearly with coverage because of adsorbate-adsorbent interaction. It gives adsorption with uniform distribution of binding energies. The linearized form of Temkin model is given in Eq. (8) (Babarinde et al. 2016).

$$q_e = B \ln(K_T) + B \ln(C_e) \quad \text{where } B = \frac{RT}{b_T} \qquad (8)$$

Where $K_T$ is Temkin isotherm equilibrium constant (Lg$^{-1}$) related to adsorption potential and B indicates heat of sorption that gives adsorbate-adsorbent interaction, $b_T$ is a dimensionless Temkin isotherm constant, $R$ is ideal gas constant (8.314 J mol$^{-1}$ K$^{-1}$), T is the temperature (K) (Matouq et al. 2015). The Temkin model parameters $K_T$ and $b_T$ were evaluated from the slope and intercept of the straight line of $q_e$ vs $\ln(C_e)$.

The Dubinin–Radushkevich equilibrium isotherm model (Eq. 9) is generally employed to find whether adsorption involved in the experimental data is physical or chemical and to evaluate the mean energy of sorption (Bhatti et al. 2007; Matouq et al. 2015; Saravanan et al. 2018). This model is more general than Langmuir isotherm model because in this model adsorption potential of all sites is not constant. According to Saravanan et al. (2018), the linearized form of Dubinin–Radushkevich isotherm equation is expressed as

$$\ln q_e = \ln q_m - k_{DR} \epsilon^2 \quad \text{where } \epsilon = \left[ RT \ln\left(1 + \frac{1}{C_e}\right)\right] \qquad (9)$$

$q_m$ is the theoretical sorption capacity (mg g$^{-1}$), $k_{DR}$ is Dubinin–Radushkevich constant related to mean energy of adsorption. A plot of $\ln q_e$ vs $\epsilon^2$ is used to find the values of model parameters $q_m$ and $k_{DR}$ from the slope and intercept of the curve. The mean free energy of sorption ($E_s$) using Dubinin–Radushkevich constant $k_{DR}$ can be computed from Eq. (10) (Matouq et al. 2015)

$$E_s = \frac{1}{\sqrt{2k_{DR}}} \qquad (10)$$

If $E_s < 8$ kJ mol$^{-1}$, it indicates physical adsorption and if $16$ kJ mol$^{-1}$ > $E_s$ > $8$ kJ mol$^{-1}$ shows chemical sorption or ion exchange (Babarinde et al. 2016). In our case, there is physical adsorption of Pb(II) on the surface of MOL as $E_s = 2.7$ kJ mol$^{-1}$.

Chi-squared test (Eq. 3) was also performed to evaluate the best isotherm model. The best fit was obtained again with the Freundlich model which yielded the lowest Chi-square value (1.79) as compared with Langmuir (3.69), Dubinin–Radushkevisch (22.13), and Temkin (49.81).

## Study of kinetic models for biosorption

Kinetic studies are important to understand the adsorption rate and reaction controlling parameters (Suganya and Kumar 2018b). A kinetic study was performed at different time intervals (15, 30, 60, 120, 180 min) with a fixed dosage of the biomass (0.7 g/100 mL) at an initial concentration of Pb(II) (80 mg/L) and pH 6. The kinetic experimental data were analyzed with the linearized form of kinetic models: pseudo first-order (Manzoor et al. 2013), pseudo second-order (Matouq et al. 2015), intra-particle diffusion (Okoli et al. 2017) and Elovich (Babarinde et al. 2016) models (Eq. 11–14), respectively.

$$\log (q_e - q_t) = \log q_e - \frac{k_1}{2.303} t \qquad (11)$$

$$\frac{t}{q_t} = \frac{1}{k_2 q_e^2} + \frac{1}{q_e} t \qquad (12)$$

$$q_t = k_{id} \sqrt{t} + C \qquad (13)$$

$$q_t = \frac{1}{\beta} \ln(\alpha\beta) + \frac{1}{\beta} \ln(t) \qquad (14)$$

Where $q_e$ is the equilibrium adsorption (mg/g), $q_t$ is the kinetic adsorption at time $t$ (min), $k_1$ indicates the rate constant of first order adsorption (min$^{-1}$), $k_2$ pseudo second constant (g mg$^{-1}$ min$^{-1}$), $k_{id}$ indicates intra-particle diffusion constant (mg g$^{-1}$ min$^{-1/2}$), C is a constant representing the thickness of the boundary layer (mg g$^{-1}$), $\alpha$ is initial adsorption rate (mg g$^{-1}$ min$^{-1}$), $\beta$ is the extent of surface area coverage and activation energy (g mg$^{-1}$).

The parameters of the aforementioned kinetic models were measured from plots of linearized form of the models (Table 1). The pseudo first rate order constants ($k_1$ and $q_e$) were determined from the slope and intercept of $\log(q_e - q_t)$ vs $t$ and pseudo second order constants ($k_2$ and $q_e$) were calculated from the slope and intercept of $\frac{t}{q_t}$ vs $t$. Similarly, parameters ($k_{id}$ and $C$) of intra-particle diffusion model were calculated from the slope and intercept of $q_t$ vs $\sqrt{t}$ while Elovich model parameters ($\alpha$ and $\beta$) were found from the slope and intercept of $q_t$ vs $ln(t)$. In batch scale experiments, it is expected that film diffusion and intra-particle diffusion may be the rate determining step (Shah *et al.* 2018). However, on the basis of adsorption capacity and coefficient of determination ($R^2$), pseudo second order kinetic model gave best fit ($R^2 = 0.996$) while pseudo first order ($R^2 = 0.975$) and Elovich model ($R^2 = 0.940$) adequately fitted the experimental data (Table 1 and Figure 4(b)). The values of pseudo first order and second rate constants ($0.121\,\text{min}^{-1}$, $0.005\,\text{min}^{-1}$) are lower than the values calculated by Saravanan *et al.* (2018) for the removal of Zn using surface modified *caryota urens* seeds which demonstrates their higher adsorption potential than the present study.

Intra-particle diffusion model is least fitted ($R^2 = 0.84$) with the kinetic experimental data for Pb(II) sorption as the curve between $q_t$ vs $\sqrt{t}$ was not linear over the entire range of time. In was observed that Pb(II) sorption on MOL involved more than one steps and intra-particle diffusion is not the rate limiting step as per simulation results with intra-particle diffusion model (Gunasundari and Kumar 2017).

## Comparison of MOL adsorption with other parts of *Moringa oleifera* and other biosorbents

The biosorption capacities of various biosorbents and *Moringa oleifera* (pods, seeds, modified leaves, bark etc.) towards Pb(II) removal are presented in Table 2. The comparison shows that without modification of surface characteristics, MOL is relatively better biosorbent for the removal of Pb (II). So, it could be used efficiently with considerable biosorption capacity for the removal of Pb(II) and its potential can be enhanced with surface modifications or making its composites with nanomaterials.

## Conclusions

In the present study, we deeply studied biosorption mechanism, isotherms, and kinetics for the removal of Pb(II) by *Moringa oleifera* leaves (MOL). The results revealed that Pb(II) removal efficiency (%) is decreased with increase in Pb(II) concentration (5–160 mg/L) due to a higher number of metals ions at a higher concentration than the active sites at a given dosage. Biosorption involves fast kinetics and is increased with the dosage of the adsorbent due to more number of active adsorption sites at a higher dosage. Maximum biosorption of Pb(II) ions per unit mass of the adsorbent (45.83 mg/g) was obtained at dosage 0.15 g/ 100 mL while maximum Pb(II) was removed (98.6%) at 1.0 g

**Table 2.** Comparison of Pb(II) biosorption with other parts of *Moringa oleifera* and other biosorbents (activated and raw).

| Biomass | q (mg/g) | Reference |
| --- | --- | --- |
| Raw biomass | | |
| *Asplenium nidus* | 9.15 | Dissanayake et al. 2016 |
| *Moringa oleifera* seed powder | 15.38 | Adhiambo et al. 2015 |
| Cuttlebone | 45.9 | Dobaradaran et al. 2017 |
| Lemon grass | 152.67 | Babarinde et al. 2016 |
| *Moringa oleifera* seeds | 0.54 | Aziz et al. 2016 |
| *Nymphoides Peltata* | 82.9 | Tseveendorj et al. 2018 |
| Fern tree | 40 | Ho et al. 2004 |
| *Moringa oleifera* leaves | 45.83 | This study |
| Activated biomass | | |
| Apple juice | 108 | Heraldy et al. 2018 |
| Tomato waste | 158 | Heraldy et al. 2018 |
| Lysinibacillus | 40 | Mathivanan et al. 2018 |
| Native kernel of *Mangifera indica* | 142.85 | Nadeem et al. 2016 |
| Native seed of *Mangifera indica* | 212 | Nadeem et al. 2016 |
| Mango peel | 99.05 | Iqbal et al. 2009 |
| Jatoba Fruit shell | 48.75 | Souza et al. 2017 |
| *Solanum melongena* leaf | 71.42 | Yuvaraja et al. 2014 |
| Modified pomegranate waste | 111.55 | Alam et al. 2012 |

adsorbent dosage. The presence of coexisting ions reduced biosorption and removal of Pb(II) (8.5% and 5%) in groundwater samples GW1, GW2, respectively. In the desorption study, the removal of Pb(II) by MOL decreased from 97% to 89% after five biosorption/desorption cycles with 0.3 M HCl. Freundlich model gave a better fit of isothermal experimental results while kinetic behavior was best explained by the pseudo-second-order kinetic model for the biosorption of Pb (II). The FTIR spectra confirmed that –OH, C–H, –C–O, –C = O, and –O–C functional groups were involved in the biosorption of Pb(II) on the surface of MOL and proved MOL as a low cost and environment-friendly material. It can be concluded from the results that the dried biomass of MOL has a great affinity towards the heavy metal removal particularly Pb (II). Hence, it can be effectively utilized for the removal of heavy metals from the various industrial wastes containing heavy metals.

## References

Abid M, Niazi NK, Bibi I, Farooqi A, Ok YS, Kunhikrishnan A, Ali F, Ali S, Igalavithana AD, Arshad M. 2016. Arsenic(V) biosorption by charred orange peel in aqueous environments. *Int J Phytoremed.* **18**(5):442–449. doi:10.1080/15226514.2015.1109604

Acharya J, Sahu J, Mohanty C, Meikap B. 2009. Removal of lead (II) from wastewater by activated carbon developed from Tamarind wood by zinc chloride activation. *Chem Eng J.* **149**(1–3):249–262. doi:10.1016/j.cej.2008.10.029

Adeogun A, Bello O, Adeboye M. 2010. Biosorption of lead ions on biosorbent prepared from plumb shells (Spondias mombin): kinetics and equilibrium studies. *Pak J Sci Ind Res.* **53**:246–251.

Adhiambo OR, Lusweti KJ, Moranga GZ. 2015. Biosorption of $Pb^{2+}$ and $Cr^{2+}$ using *Moringa oleifera* and their adsorption isotherms.. *Sci J Anal Chem*. 3(6):100–108. doi:10.11648/j.sjac.20150306.14

Ahalya N, Kanamadi RD, Ramachandra TV. 2005. Biosorption of chromium from aqeous solution using husk of Bengal gram. *Electron J Biotechnol*. 8:258–264. doi:10.2225/vol8-issue3-fulltext-10

Ahmad I, Akhtar MJ, Jadoon IBK, Imran M, Imran M, Ali S. 2017. Equilibrium modeling of cadmium biosorption from aqueous solution by compost. *Environ Sci Pollut Res Int*. 24(6):5277–5284. doi:10.1007/s11356-016-8280-y

Ahmed S, Mustafa T. 2008. Biosorption of cadmium (II) from aqueous solution by red algae (*Ceramium virgatum*) equilibrium, kinetic and thermodynamic studies. *J Hazard Mater*. 157:448–454.

Al-Ghouti MA, Khraisheh MAM, Allen SJ, Ahmad MN. 2003. The removal of dyes from textile wastewater: a study of the physical characteristics and adsorption mechanisms of diatomaceous earth. *J Environ Manag*. 69(3):229–240. doi:10.1016/j.jenvman.2003.09.005

Alam M, Nadeem R, Jilani MI. 2012. Pb (II) removal from wastewater using Pomegranate waste biomass. Int J Chem Biochem Sci. 1:24–29.

Ali RM, Hamad HA, Hussein MM, Malash GF. 2016. Potential of using green adsorbent of heavy metal removal from aqueous solutions: adsorption kinetics, isotherm, thermodynamic, mechanism and economic analysis. *Ecol Eng*. 91:317–332. doi:10.1016/j.ecoleng.2016.03.015

Aliabadi HM, Saberikhah E, Pirbazari AE, Khakpour R, Alipour H. 2018. Triethoxysilylpropylamine modified alkali treated wheat straw: an efficient adsorbent for methyl orange adsorption. *Cellulose Chem Technol*. 52:129–140.

Anastopoulos I, Massas I, Ehaliotis C. 2013. Composting improves biosorption of $Pb^{2+}$ and $Ni^{2+}$ by renewable lignocellulosic materials. Characteristics and mechanisms involved. *Chem Eng J*. 231:245–254. doi:10.1016/j.cej.2013.07.028

Anwar F, Latif S, Ashraf M, Gilani AH. 2007. *Moringa oleifera*: a food plant with multiple medicinal uses. *Phytother Res*. 21(1):17–25. doi:10.1002/ptr.2023

Araújo CST, Alves VN, Rezende HC, Almeida ILS, de Assunção RMN, Tarley CRT, Segatelli MG, Coelho NMM. 2010. Characterization and use of *Moringa oleifera* seeds as biosorbent for removing metal ions from aqueous effluents. *Water Science and Technology*. 62(9):2198–2203. doi: doi:10.2166/wst.2010.419.

Araújo CST, Carvalho DC, Rezende HC, Almeida ILS, Coelho LM, Coelho NMM, Marques TL, Alves VN. 2013. Bioremediation of waters contaminated with heavy metals using Moringa oleifera seeds as biosorbent. In: Patil Y, Rao P, editors. Applied bioremediation-active and passive approaches. Croácia: InTech Open Science. p. 225–253.

Aziz NAA, Jayasuriya N, Fan L. 2016. Adsorption study on *Moringa oleifera* seeds and Musa cavendish as natural water purification agents for removal of Lead, Nickel and Cadmium from drinking water. In IOP Conference Series: Materials Science and Engineering, Institute of Physics Publishing.

Babarinde A, Ogundipe K, Sangosanya KT, Akintola BD, Hassan AOE. 2016. Comparative study on the biosorption of Pb(II), Cd (II) and Zn (II) using Lemon grass (*Cymbopogon citratus*): kinetics, isotherms and thermodynamics. *Chem Int*. 2(2):89–102.

Balaria A, Schiewer S, Schiewer S. 2008. Assessment of biosorption mechanism for Pb(II) binding by citrus pectin. *Sep Purif Technol*. 63(3):577–581. doi:10.1016/j.seppur.2008.06.023

Bello OS, Ahmad MA. 2011. Response surface modeling and optimization of Remazol Brilliant Blue reactive dye removal using periwinkle shell-based activated carbon. *Sep Sci Technol*. 46(15):2367–2379. doi:10.1080/01496395.2011.595756

Benguella B, Benaissa H. 2002. Cadmium removal from aqueous solutions by chitin: kinetic and equilibrium studies. *Water Res*. 36(10):2463–2474. doi:10.1016/S0043-1354(01)00459-6

Bhatti HN, Mumtaz B, Hanif MA, Nadeem R. 2007. Removal of Zn (II) ions from aqueous solution using *Moringa oleifera* Lam.(horseradish tree) biomass. *Proc Biochem*. 42(4):547–553. doi:10.1016/j.procbio.2006.10.009

Bilal M, Shah JA, Ashfaq T, Gardazi SMH, Tahir AA, Pervez A, Haroon H, Mahmood Q. 2013. Waste biomass adsorbents for copper removal from industrial wastewater-a review. *J Hazard Mater*. 263:322–333. doi:10.1016/j.jhazmat.2013.07.071

Bueno BYM, Torem ML, Molina F, De Mesquita LMS. 2008. Biosorption of lead (II), chromium (III) and copper (II) by R. opacus: equilibrium and kinetic studies. *Min Eng*. 21(1):65–75. doi:10.1016/j.mineng.2007.08.013

Carolin CF, Kumar PS, Saravanan A, Joshiba GJ, Naushad M. 2017. Efficient techniques for the removal of toxic heavy metals from aquatic environment: a review. *J Environ Chem Eng*. 5(3):2782–2799. doi:10.1016/j.jece.2017.05.029

Chandrasekhar K, Kamala CT, Chary NS, Anjaneyulu Y. 2001. Removal of heavy metals using a plant biomass with reference to environmental control. *Int J Miner Process*. 68:37–45.

Demirbas A. 2008. Heavy metal adsorption onto agro-based waste materials: a review. *J Hazard Mater*. 157(2-3):220–229. doi:10.1016/j.jhazmat.2008.01.024

Dissanayake DMREA, Wijesinghe WMKEH, Iqbal SS, Priyantha N, Iqbal MCM. 2016. Isotherm and kinetic study on Ni (II) and Pb(II) biosorption by the fern Asplenium nidus L. *Ecol Eng*. 88:237–241. doi:10.1016/j.ecoleng.2015.12.028

Dobaradaran S, Kakuee M, Pazira AR, Keshtkar M, Khorsand M. 2015. Fluoride removal from aqueous solutions using *Moringa oleifera* seed ash as an environmental friendly and cheap biosorbent. *Fresenius Environ Bull*. 24(4):1269–1274.

Dobaradaran S, Nabipour I, Keshtkar M, Ghasemi FF, Nazarialamdarloo T, Khalifeh F, Poorhosein M, Abtahi M, Saeedi R. 2017. Self-purification of marine environments for heavy metals: a study on removal of lead(II) and copper(II) by cuttlebone. *Water Sci Technol*. 75(2):474–481. doi:10.2166/wst.2016.533

Gao A, Xie K, Song X, Zhang K, Hou A. 2017. Removal of the heavy metal ions from aqueous solution using modified natural biomaterial membrane based on silk fibroin. *Ecol Eng*. 99:343–348. doi:10.1016/j.ecoleng.2016.11.008

Guiza S. 2017. Biosorption of heavy metal from aqueous solution using cellulosic waste orange peel. *Ecol Eng*. 99:134–140. doi:10.1016/j.ecoleng.2016.11.043

Gunasundari E, Kumar S. 2017. Adsorption isotherm, kinetics and thermodynamic analysis of Cu (II) ions onto the dried algal biomass (*Spirulina platensis*). *J Ind Eng Chem*. 56:129–144.

Hameed B, Din AM, Ahmad A. 2007. Adsorption of methylene blue onto bamboo-based activated carbon: kinetics and equilibrium studies. *J Hazard Mater*. 141(3):819–825. doi:10.1016/j.jhazmat.2006.07.049

Heraldy E, Lestari WW, Permatasari D, Arimurti DD. 2018. Biosorbent from tomato waste and apple juice residue for lead removal. *J Environ Chem Eng*. 6(1):1201–1208. doi:10.1016/j.jece.2017.12.026

Ho YS, Chiu WT, Hsu CS, Huang CT. 2004. Sorption of lead ions from aqueous solution using tree fern as a sorbent. *Hydrometallurgy*. 73(1-2):55–61. doi:10.1016/j.hydromet.2003.07.008

Igbal M, Edyvean RGJ. 2004. Biosorption of lead, copper and zinc ions on loofa immobilized biomass of Phanerochaete chysosporium. *Miner Eng*. 17:217–223. doi:10.1016/j.mineng.2003.08.014

Imran M, Suddique M, Shah G, Ahmad I, Murtaza B, Shah N, Mubeen M, Ahmad S, Zakir A, Schotting R. 2018. Kinetic and equilibrium studies for cadmium biosorption from contaminated water using Cassia fistula biomass. Int J Environ Sci Tech [in press]. 1–10.

Iqbal S, Bhanger MI. 2006. Effect of season and production location on antioxidant activity of *Moringa oleifera* leaves grown in Pakistan. *J Food Comp Anal*. 19(6–7):544–551. doi:10.1016/j.jfca.2005.05.001

Iqbal M, Saeed A, Zafar SI. 2009. FTIR spectrophotometry, kinetics and adsorption isotherms modeling, ion exchange, and EDX analysis for understanding the mechanism of $Cd^{2+}$ and $Pb^{2+}$ removal by mango peel waste. *J Hazard Mat*. 164(1):161–171. doi:10.1016/j.jhazmat.2008.07.141

John E. 2011. An A-Z Guide to the elements. Oxford, England: Oxford University Press.

Kamal MHMA, Azira WMKWK, Kasmawati M, Haslizaidi Z, Saime WNW. 2010. Sequestration of toxic Pb(II) ions by chemically treated

rubber (*Hevea brasiliensis*) leaf powder. *J Environ Sci*. 22(2): 248–256. doi:10.1016/S1001-0742(09)60101-7

Kaveeshwar AR, Ponnusamy SK, Revellame ED, Gang DD, Zappi ME, Subramaniam R. 2018. Pecan shell based activated carbon for removal of iron (II) from fracking wastewater: adsorption kinetics, isotherm and thermodynamic studies. *Proc Safety and Environ Protect*. 114:107–122. doi:10.1016/j.psep.2017.12.007

Kołodyńska D, Krukowska J, Thomas P. 2017. Comparison of sorption and desorption studies of heavy metal ions from biochar and commercial active carbon. *Chem Eng J*. 307:353–363. doi:10.1016/j.cej.2016.08.088

Liu X, Liu B, Wang Z, Zhang B, Zhang Z. 2008. Oriented vaterite CaCO$_3$ tablet-like arrays mineralized at air/water interface through cooperative regulation of polypeptide and double hydrophilic block copolymer. *J Phys Chem C*. 112(26):9632–9636. doi:10.1021/jp8017088

Manzoor Q, Nadeem R, Iqbal M, Saeed R, Ansari TM. 2013. Organic acids pretreatment effect on *Rosa bourbonia* phyto-biomass for removal of Pb(II) and Cu(II) from aqueous media. *Bioresour Technol*. 132:446–452. doi:10.1016/j.biortech.2013.01.156

Mathivanan K, Rajaram R, Annadurai G. 2018. Biosorption potential of *Lysinibacillus fusiformis* KMNTT-10 biomass in removing lead (II) from aqueous solutions. *Sep Sci Technol*. 53:1991–2003. doi:10.1080/01496395.2018.1442863

Matouq M, Jildeh N, Qtaishat M, Hindiyeh M, Syouf MQA. 2015. The adsorption kinetics and modeling for heavy metals removal from wastewater by *Moringa* pods. *J Environ Chem Eng*. 3(2):775–784. doi:10.1016/j.jece.2015.03.027

Meseguer VF, Ortuño JF, Aguilar MI, Pinzón-Bedoya ML, Lloréns M, Sáez J, Pérez-Marín AB. 2016. Biosorption of cadmium (II) from aqueous solutions by natural and modified non-living leaves of *Posidonia oceanica*. *Environ Sci Pollut Res Int*. 23(23):24032–24046. doi:10.1007/s11356-016-7625-x

Mirghaffari N, Moeini E, Farhadian O. 2015. Biosorption of Cd and Pb ions from aqueous solutions by biomass of the green microalga, *Scenedesmus quadricauda*. *J Appl Phycol*. 27(1):311–320. doi:10.1007/s10811-014-0345-z

Nadeem R, Manzoor Q, Iqbal M, Nisar J. 2016. Biosorption of Pb(II) onto immobilized and native *Mangifera indica* waste biomass. *J Ind Eng Chem*. 35:185–194. doi:10.1016/j.jiec.2015.12.030

Niazi NK, Bibi I, Shahid M, Ok YS, Shaheen SM, Rinklebe J, Wang H, Murtaza B, Islam E, Nawaz MF, Lüttge A. 2018. Arsenic removal by Japanese oak wood biochar in aqueous solutions and well water: investigating arsenic fate using integrated spectroscopic and microscopic techniques. *Sci Total Environ*. 621:1642–1651. doi:10.1016/j.scitotenv.2017.10.063

Nithya K, Sathish A, Kumar PS, Ramachandran T. 2018. Fast kinetics and high adsorption capacity of green extract capped superparamagnetic iron oxide nanoparticles for the adsorption of Ni (II) ions. *J Ind Eng Chem*. 59:230–241. doi:10.1016/j.jiec.2017.10.028

Okoli CP, Diagboya PN, Anigbogu IO, Olu-Owolabi BI, Adebowale KO. 2017. Competitive biosorption of Pb(II) and Cd (II) ions from aqueous solutions using chemically modified moss biomass (*Barbula lambarenensis*). *Environ Earth Sci*. 76:33. doi:10.1007/s12665-016-6368-9

Pappalardo L, Jumean F, Abdo N. 2010. Removal of cadmium, copper, lead and nickel from aqueous solution by White, Yellow, and Red United Arab Emirates sand. *Am J Env Sci*. 6:41–44. doi:10.3844/ajessp.2010.41.44

Raoof A, Hassanizadeh SM, Leijnse A. 2010. Upscaling transport of adsorbing solutes in porous media: pore-network modeling. *Vadosage Zone J*. 9(3):624–636. doi:10.2136/vzj2010.0026

Ravikumar K, Sheeja AK. 2013. Heavy metal removal from water using Moringa oleifera seed coagulant and double filtration. Paper presentd at: International Conference on Innovations in Civil Engineering, Kerala, India.

Reddy DHK, Ramana DKV, Seshaiah K, Reddy AVR. 2011. Biosorption of Ni(II) from aqueous phase by *Moringa oleifera* bark. *Desalination*. 268(1–3):150. doi:10.1016/j.desal.2010.10.011

Reddy DHK, Seshaiah K, Reddy AVR, Lee SM. 2012. Optimization of Cd (II), Cu (II) and Ni (II) biosorption by chemically modified *Moringa oleifera* leaves powder. *Carbohydrate Polymers*. 88(3): 1077–1086. doi:10.1016/j.carbpol.2012.01.073

Saeed A, Iqbal M. 2003. Bioremoval of cadmium from aqueous solution by black gram husk (*Cicer arientinum*). *Water Res*. 37(14): 3472–3480. doi:10.1016/S0043-1354(03)00175-1

Saha GC, Hoque MIU, Miah MAM, Holze R, Chowdhury DA, Khandaker S, Chowdhury S. 2017. Biosorptive removal of lead from aqueous solutions onto Taro (*Colocasiaesculenta* (L.) Schott) as a low cost bioadsorbent: characterization, equilibria, kinetics and biosorption-mechanism studies. *J Environ Chem Eng*. 5(3):2151–2162. doi: doi:10.1016/j.jece.2017.04.013.

Sarada B, Prasad MK, Kumar KK, Murthy CVR. 2014. Potential use of *Caulerpa fastigiata* biomass for removal of lead: kinetics, isotherms, thermodynamic, and characterization studies. *Environ Sci Pollut Res*. 21(2):1314–1325. doi:10.1007/s11356-013-2008-z

Saravanan A, Kumar PS, Renita AA. 2018. Hybrid synthesis of novel material through acid modification followed ultrasonication to improve adsorption capacity for zinc removal. *J Cleaner Prod*. 172: 92–105. doi:10.1016/j.jclepro.2017.10.109

Shah GM, Nasir M, Imran M, Bakhat HF, Rabbani F, Sajjad M, Farooq ABU, Ahmad S, Song L. 2018. Biosorption potential of natural, pyrolysed and acid-assisted pyrolysed sugarcane bagasse for the removal of lead from contaminated water. *Peer J*. 6:e5672. doi: 10.7717/peerj.5672

Shahid M, Khalid M, Dumat C, Khalid S, Niazi NK, Imran M, Bibi I, Ahmad I, Hammad HM, Tabassum RA. 2018. Arsenic level and risk assessment of groundwater in Vehari, Punjab Province, Pakistan. *Expo Health*. 10:229–239. doi:10.1007/s12403-017-0257-7

Shakoor MB, Niazi NK, Bibi I, Rahman MM, Naidu R, Dong Z, Shahid M, Arshad M. 2015. Unraveling health risk and speciation of arsenic from groundwater in rural areas of Punjab, Pakistan. *Int J Environ Res Public Health*. 12(10):12371–12390. doi:10.3390/ijerph121012371

Sheng PX, Tan LH, Chen JP, Ting YP. 2005. Biosorption performance of two brown marine algae for removal of chromium and cadmium. *J of Dis ScI and Technol*. 25(5):679–686. doi:10.1081/DIS-200027327

Shim J, Kim J, Shea PJ, Oh BT. 2015. Biosorption of cadmium by *Citrobacter* sp. JH 11-2 isolated from mining site soil. *Sep Sci Technol*. 50(14):2134–2141.

Soliman EM, Ahmed SA, Fadl AA. 2011. Reactivity of sugar cane bagasse as a natural solid phase extractor for selective removal of Fe (III) and heavy-metal ions from natural water samples. *Arabian J Chem*. 4(1):63–70. doi:10.1016/j.arabjc.2010.06.021

Souza IPAF, Cazetta AL, Pezoti O, Almeida VC. 2017. Preparation of biosorbents from the Jatoba (*Hymenaea courbaril*) fruit shell for removal of Pb(II) and Cd (II) from aqueous solution. *Environ Mon Assess*. 189(12):632. doi:10.1007/s10661-017-6330-7

Sreelatha S, Padma PR. 2009. Antioxidant activity and total phenolic content of *Moringa oleifera* leaves in two stages of maturity. *Plant Foods Hum Nutr*. 64(4):303 doi:10.1007/s11130-009-0141-0

Subramani SE, Thinakaran N. 2017. Isotherm, kinetic and thermodynamic studies on the adsorption behaviour of textile dyes onto chitosan. *Proc Saf Environ Prot*. 106:1–10.

Suganya S, Kumar PS. 2018a. Evaluation of environmental aspects of brew waste-based carbon production and its disposal scenario. *J Cleaner Prod*. 202:244–252. doi:10.1016/j.jclepro.2018.08.143

Suganya S, Kumar S. 2018b. Influence of ultrasonic waves on preparation of active carbon from coffee waste for the reclamation of effluents containing Cr (VI) ions. *J Ind Eng Chem*. 60:418–430.

Sulaymon AH, Mohammed AA, Al-Musawi TJ. 2013. Equilibrium, kinetic, and thermodynamic biosorption of Pb (II), Cr (III), and Cd (II) ions by dead anaerobic biomass from synthetic wastewater. *Environ Sci Pollut Res*. 20(5):3011–3023. doi:10.1007/s11356-012-1208-2

Tarley CRT, Arruda MAZ. 2004. Biosorption of heavy metals using rice milling by-products. Characterisation and application for removal of metals from aqueous effluents. *Chemosphere*. 54:987–995. doi:10.1016/j.chemosphere.2003.09.001

Tavares FO, Pinto LAM, Bassetti FJ, Vieira MF, Bergamasco R, Vieira AMS. 2017. Environmentally friendly biosorbents (husks, pods and seeds) from *Moringa oleifera* for Pb(II) removal from contaminated water. *Environ Technol*. **38**:3145–3155. doi:10.1080/09593330.2017.1290150

Tofan L, Paduraru C, Volf I, Toma O. 2011. Waste of rapeseed from biodiesel production as a potential biosorbent for heavy metal ions. *Bioresources*. **6**(4):3727–3741.

Tseveendorj E, Enkhdul T, Lin S, Dorj D, Oyungerel S, Soyol-Erdene TO. 2018. Biosorption of lead (II) from an aqueous solution using biosorbents prepared from water plants. *Mong J Chem*. **18**(44): 52–61.

Vilvanathan S, Shanthakumar S. 2015. Biosorption of Co(II) ions from aqueous solution using *Chrysanthemum indicum*: Kinetics, equilibrium and thermodynamics. *Process Saf Environ Prot*. **96**:98–110. doi:10.1016/j.psep.2015.05.001

Wang JL, Chen C. 2009. Biosorbents for heavy metals removal and their future a review. *Biotechnol Advance*. **52**:195–226.

Xiong TT, Dumat C, Pierart A, Shahid M, Kang Y, Li N, Bertoni G, Laplanche C. 2016. Measurement of metal bioaccessibility in vegetables to improve human exposure assessments: field study of soil–plant–atmosphere transfers in urban areas, South China. *Environ Geochem Health*. **38**(6):1283–1301. doi:10.1007/s10653-016-9796-2

Yao Z, Shi Y, Li J, Pan L, Qiu H, Wang X. 2012. Electrical characterization of back-gated bi-layer $MoS_2$ field-effect transistors and the effect of ambient on their performances. *Appl Phys Lett*. **100**:123104.

Yuvaraja G, Krishnaiah N, Subbaiah MV, Krishnaiah A. 2014. Biosorption of Pb(II) from aqueous solution by *Solanum melongena* leaf powder as a low-cost biosorbent prepared from agricultural waste. *Coll Surf B Biointer*. **114**:75–81. doi:10.1016/j.colsurfb.2013.09.039